

Transport properties of $\text{InAs}_x\text{Sb}_{1-x}$ ($0 \leq x \leq 0.55$) on InP grown by molecular-beam epitaxy

S. Tsukamoto, P. Bhattacharya, Y. C. Chen, and J. H. Kim

Solid State Electronics Laboratory, Department of Electrical Engineering and Computer Science, The University of Michigan, Ann Arbor, Michigan 48109-2122

(Received 11 December 1989; accepted for publication 12 February 1990)

Molecular-beam epitaxy has been successfully used to grow $\text{InAs}_x\text{Sb}_{1-x}$ on InP substrates with good electrical characteristics. The samples are all n type with electron concentrations varying in the range $(3-9) \times 10^{15} \text{ cm}^{-3}$. The mobilities are high (70 000 and 110 000 $\text{cm}^2/\text{V s}$ at 300 and 77 K, respectively) in InSb and the alloys. More importantly, the mobilities remain high at the low temperatures in the alloys also, without any type conversion. The mobility data have been analyzed taking into account the appropriate scattering mechanisms. The alloy scattering potential in $\text{InAs}_{0.24}\text{Sb}_{0.76}$ is estimated to be 0.3 V.

I. INTRODUCTION

The Sb-containing alloys, their heterostructures and superlattices, are becoming increasingly important for long-wavelength optoelectronic and cryogenic electronic device applications. In particular, the $\text{InAs}_x\text{Sb}_{1-x}$ alloys produce the lowest band gap—100 meV in $\text{InAs}_{0.4}\text{Sb}_{0.6}$ at 300 K—in the family of III-V compounds. They are therefore suitable for infrared detectors and sources operating at wavelengths in the 3–5 and 8–12 μm windows where the atmospheric absorption goes to a minimum.^{1,2} Two shortcomings that have been detrimental to the development of high-quality materials are the prediction of a miscibility gap in the midregion of the composition range and the nonavailability of suitable lattice-matched substrates. Therefore equilibrium growth techniques can lead to severe phase separation and clustering. Nonequilibrium techniques of crystal growth, such as molecular-beam epitaxy, become very useful in this case. The second drawback presents advantages and disadvantages. If the antimonides are grown on GaAs or InP, resulting in 7%–15% mismatch, the epitaxial layer has a large density of threading dislocations. However, if with appropriate growth techniques good quality crystals can be grown, this allows the possibility of integrating the Sb-containing devices with GaAs- and InP-based technologies.

The best carrier mobilities have been measured in bulk InSb, with a room-temperature mobility of 60 000 and that of 150 000 cm^2/V at 200 K.³ The alloys have been grown by Abrokwhah and Gershenzon⁴ by LPE, and several groups of authors^{5–8} have grown them by molecular-beam epitaxy (MBE). Although high mobilities are measured at room temperature, there is a severe degradation in the mobility values at low temperatures accompanied by a type conversion, both of which have been attributed to the high density of defects and Si-related autocompensation. In spite of these drawbacks, we have recently grown InSb on InP and have measured mobilities of 70 000 and 110 000 $\text{cm}^2/\text{V s}$ at 300 and 77 K, respectively. The unintentional doping in the 5–10- μm -thick layers was n -type with $n \approx (3-5) \times 10^{15} \text{ cm}^{-3}$, and remained n type down to temperatures as low as 13 K. It is important to achieve good transport properties in the ter-

nary alloys also at low temperatures, since most electronic device applications are being envisioned at these temperatures. We report here the MBE growth of $\text{InAs}_x\text{Sb}_{1-x}$ ($0 \leq x \leq 0.55$) alloys on InP substrates and their morphological, structural, and electrical properties.

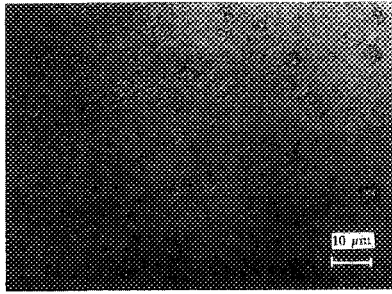
II. MOLECULAR-BEAM EPITAXIAL GROWTH

Heteroepitaxial $\text{InAs}_x\text{Sb}_{1-x}$ layers ($0 \leq x \leq 0.55$) were grown on Fe-doped (100)InP (Crystacomm) substrates in a RIBER 2300P MBE system. Elemental arsenic and antimony were used as the group V sources, producing predominantly As_4 and Sb_4 species. The InP substrates were prepared by standard solvent degreasing and transferred into the growth chamber. After oxide desorption at $\sim 520^\circ\text{C}$ under an As_4 overpressure (1.5×10^5 Torr), the growth of InAsSb was initiated at substrate temperatures in the range 350–500 $^\circ\text{C}$, as measured by an infrared pyrometer. The growth rate varied in the range 0.8–1.0 $\mu\text{m}/\text{h}$ and the flux ratio $J_{\text{Sb}_4}/J_{\text{In}}$ was varied in the range 0.3–4.0. It is to be noted that we did not initiate growth at either a low temperature (300 $^\circ\text{C}$) or low growth rate (0.1 $\mu\text{m}/\text{h}$) as was recently reported by Davis and Thompson.⁹ The thickness of these directly grown layers varied in the range of 1.0–14.0 μm .

In situ examination of the crystalline nature of growth was done by reflection high-energy electron diffraction (RHEED) measurements with 10-keV electron beams along the (110) azimuth. Our observations were essentially the same as those in previous reports.¹⁰ The observed spotty nature of the RHEED pattern at the initiation of growth indicates a three-dimensional growth mode resulting from the large lattice mismatch. After growth of a few hundred angstroms, the spots change to streaks with a (1×3) reconstruction, indicating continuous coverage and smoothening of the growth front.

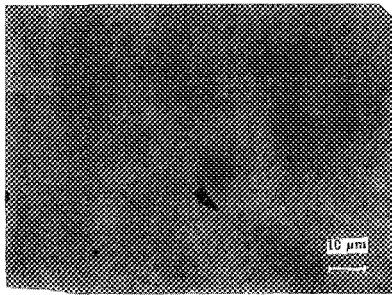
The surface morphologies of 6- μm -thick alloy films grown on 100 InP substrates, as observed under a Nomarski phase contrast microscope, are shown in Fig. 1. As the As content in the film increases, rectangular features, 5–10 μm on a side, are seen clearly. These features have been observed before and stepped growth has been suggested as a possible

T_g = 400°C
 J_{Sb₄}/J_{In} = 1.82
 t = 6.4 μm



(a) x = 0.14

T_g = 370°C
 J_{Sb₄}/J_{In} = 1.07
 t = 6.4 μm



(b) x = 0.03

FIG. 1. Observed surface morphology of (a) InAs_{0.14}Sb_{0.86} and (b) InAs_{0.03}Sb_{0.97} on InP under Nomarski phase contrast microscope.

origin.¹¹ It should be noted, however, that 5–10 μm is greater than the electron mean free path and therefore electron transport may not be affected. But these features may have important effects on minority carriers through trapping. In order to investigate the microcrystalline quality of the films we have made single-crystal x-ray diffraction measurements using the Cu *k*α₁ and *k*α₂ lines. The diffraction patterns are shown in Fig. 2. It is clear that higher As content leads to a broadening of the linewidth, indicating a deterioration in the crystalline quality. Typical linewidths vary from 1 mrad in InAs_{0.34}Sb_{0.66}.

Figure 3 shows the measured variation in alloy composition as a function of growth temperature for fixed beam equivalent pressures (BEP) of In, As₄, and Sb₄. Since the dissociation energy of Sb₄ is significantly lower than that of As₄ at lower temperatures, it incorporates preferentially over As₄. Therefore, almost all the incident Sb₄ flux is incorporated. The dominance of Sb₄ decreases rapidly at higher temperatures, where surface dissociations of arsenic becomes more important. At higher temperatures, both Sb₄ and As₄ incorporation rates decrease, showing a saturation effect.

III. ELECTRICAL TRANSPORT PROPERTIES: RESULTS AND DISCUSSION

Hall measurements were made in the temperature range of 77–300 K in a variable temperature closed cycle cryostat under a magnetic field of 0.3 T. The measured mobilities in the undoped InSb and InAsSb films, with thicknesses varying between 1.6–10.0 μm are shown in Fig. 4. All the samples

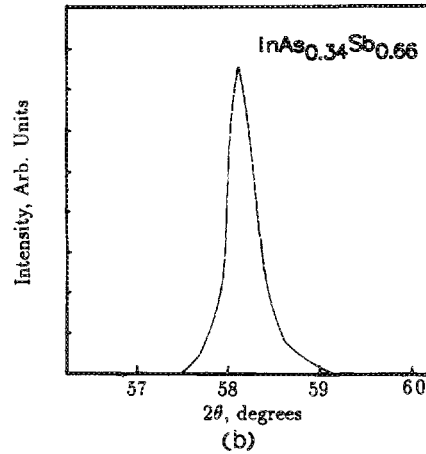
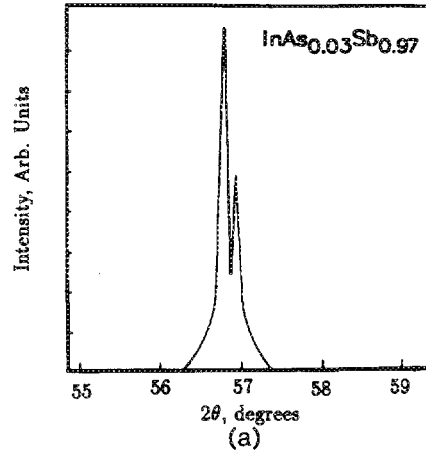


FIG. 2. Single-crystal x-ray diffraction patterns of (a) InAs_{0.3}Sb_{0.97}, and (b) InAs_{0.34}Sb_{0.66} on InP. The peaks corresponding to Cu*k*α₁ and *k*α₂ are well resolved in (a).

are *n* type. The mobility in InSb is 70 000 cm²/V s, and it rapidly drops with alloying, probably due to a combination of increased lattice mismatch and clustering effects. However, the mobility values compare very favorably with InAs_xSb_{1-x} films grown by liquid phase epitaxy on InSb substrates. This also indicates that clustering effects rather

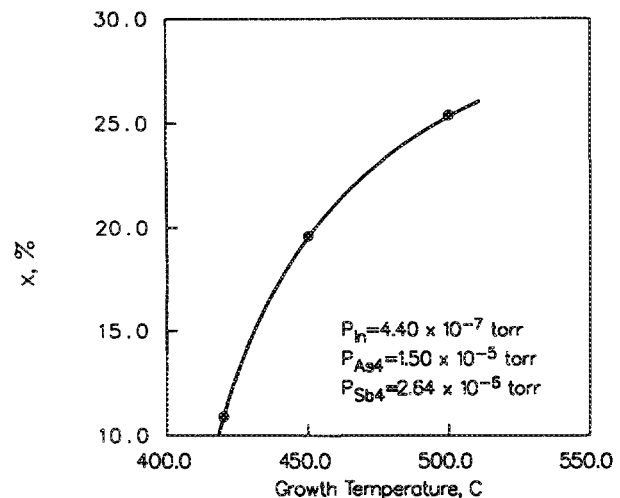


FIG. 3. Variation in InAs_xSb_{1-x} alloy composition with growth temperature for fixed beam equivalent pressures of In, As₄, and Sb₄ fluxes.

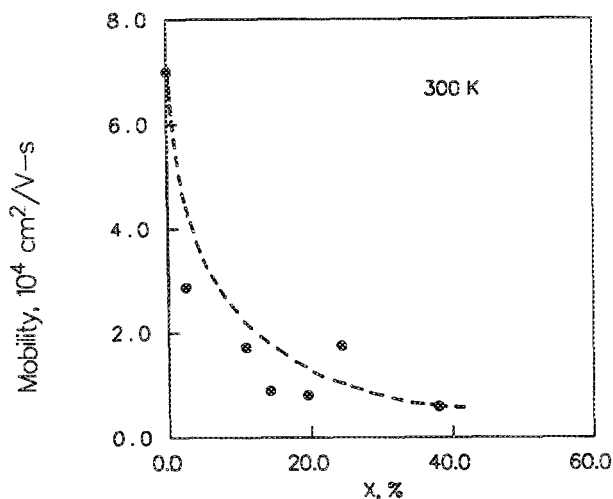


FIG. 4. Measured electron mobility at 300 K as a function of alloy composition x in $\text{InAs}_x\text{Sb}_{1-x}$ grown on InP . All the samples are n type. The dashed line is a guide to the eye.

than dislocation defects are responsible for the degradation in mobility.

The measured variation of electron mobility with temperature in InSb and $\text{InAs}_{0.24}\text{Sb}_{0.76}$ are shown in Figs. 5(a) and 5(b), respectively. It is important to note that the mobility values remain high up to the lowest temperatures of measurement. This is perhaps the first time that such a behavior has been achieved in MBE grown InAsSb . The mobility data have been analyzed by taking into account acoustic and optical phonon scattering and ionized impurity scattering. In addition, alloy scattering has been included for the ternary material. The analysis includes effects of nonparabolicity and wave function mixing.¹² The mobility limited by the various scattering effects are also shown in the figures, together with the average mobility (shown by the bold lines) calculated by Matthiessen's rule. Above $\sim 200^\circ\text{C}$, the intrinsic generation of carriers gives rise to electron-hole scattering. This has been taken into account in the ionized impurity scattering formulation, and is noticed in the figures as a decrease in the calculated mobility with temperature. The effective mass values used are $\sim 0.015 m_0$ for both materials. An alloy scattering potential $\Delta U = 0.3 \text{ eV}$ was used to analyze the mobility data in the ternary material.

The compensation ratio $(N_D - N_A)/(N_D + N_A)$ obtained from the analysis is 0.5 for InSb and 0.2 for the ternary material. Temperature dependence of the Hall electron concentrations in the different samples are shown in Fig. 6. The characteristic increase of electron concentration at high temperatures is related to the intrinsic carrier generation process. The electron concentrations in the samples range from $(3-9) \times 10^{15} \text{ cm}^{-3}$, which are quite low. The data also indicate that there are no deep levels in these materials, no freezeout effects, and no type conversion.

IV. CONCLUSIONS

We have grown high-quality $\text{InAs}_x\text{Sb}_{1-x}$ ($0 \leq x \leq 0.55$) directly on InP substrates by molecular-beam epitaxy. The undoped crystals are all n type at 300 K and at lower tem-

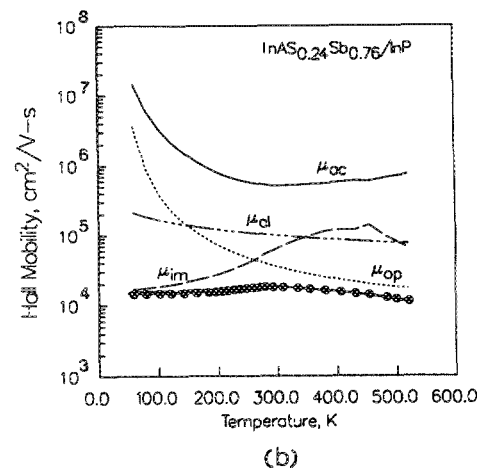
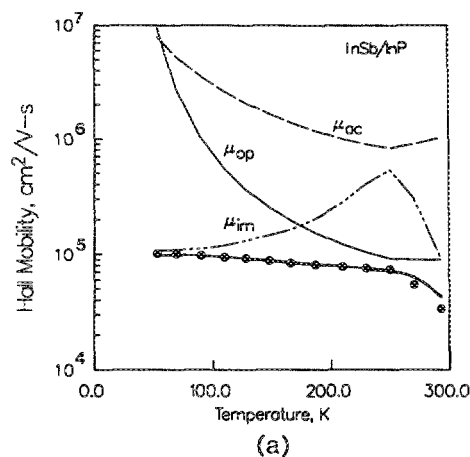


FIG. 5. Measured and calculated variation of electron mobility as a function of temperature in (a) InSb and (b) $\text{InAs}_{0.24}\text{Sb}_{0.76}$ on InP substrate. μ_{AC} , μ_{OP} , μ_{IM} , and μ_{AL} correspond to the calculated mobilities limited by acoustic phonon scattering, optical phonon scattering, ionized impurity scattering, and alloy scattering. At higher temperatures the effect of electron-hole scattering is also included.

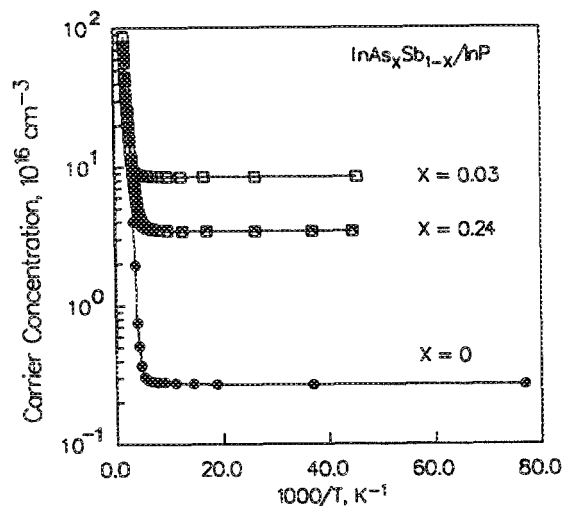


FIG. 6. Measured temperature dependence of Hall electron concentration in $\text{InAs}_x\text{Sb}_{1-x}$ on InP for various values of x .

peratures. The surface morphology and electrical transport properties are strongly dependent on the Sb₄/In flux ratio and the substrate temperature. The highest mobilities in InSb (10 μm thick) are 70 000 cm²/V s at 300 K and 110 000 cm²/V s at 77 K, and lower values are measured in the alloys. More importantly, the mobilities in the alloys also increase monotonically with lowering of temperature.

ACKNOWLEDGMENTS

The work is being supported by the National Aeronautic and Space Administration (Lewis Research Center) under Grant No. NAG-3-988 and the National Science Foundation under Grant No. ECSE-8800659.

¹G. C. Osbourn, *J. Vac. Sci. Technol. B* **2**, 2 176 (1984).

²S. R. Kurtz, I. R. Dawson, T. E. Zipperian, and S. R. Lee, *Appl. Phys.*

Lett. **52**, 1581 (1988).

³B. R. Nag, *Electron Transport in Compound Semiconductors* (Springer, Berlin, 1980), pp. 373-377; B. R. Nag and G. M. Dutta, *J. Appl. Phys.* **48**, 3621 (1977).

⁴J. K. Abrokwah and M. Gershenson, *J. Electron. Mater.* **10**, 379 (1981).

⁵G. S. Lee, Y. Lo, Y. F. Lin, S. M. Bedair, and W. D. Laidig, *Appl. Phys. Lett.* **47**, 1219 (1985).

⁶M. Y. Yen, R. People, K. W. Wecht, and A. Y. Cho, *Appl. Phys. Lett.* **52**, 489 (1988).

⁷C. G. Bethea, B. F. Levine, M. Y. Yen, and A. Y. Cho, *Appl. Phys. Lett.* **53**, 291 (1988).

⁸J. J. Chyi, S. Kalem, N. S. Kumar, C. W. Litton, and H. Morkoç, *Appl. Phys. Lett.* **53**, 1092 (1988).

⁹J. L. Davis and P. E. Thompson, *Appl. Phys. Lett.* **54**, 2235 (1989).

¹⁰G. M. Williams, C. R. Whitehouse, C. F. McConville, A. G. Cullis, T. Ashley, S. J. Courtney, and C. T. Elliott, *Appl. Phys. Lett.* **53**, 1189 (1988).

¹¹M. Yano, T. Takase, and M. Kimata, *Phys. Status Solidi A* **54**, 707 (1979).

¹²B. R. Nag and G. M. Dutta, *Phys. Status Solidi B* **71**, 401 (1975).